Chapter 2
Luminescence Properties of Thermostable Lanthanide Coordination Polymers with Intermolecular Interactions

2.1 Introduction

Luminophores with high thermal stability are promising candidates as active materials for electroluminescent (EL) devices, lasers and luminescent biosensing applications. As described in Chap. 1, lanthanide polynuclear complexes, coordination polymers, and metal-organic frameworks have been widely studied from the viewpoint of thermostable structure [1–7]. For example, Marchetti has reported a thermostable coordination polymer with Eu(III) ions and 4-acyl-pyrazolone ligands [8]. Wang has also reported that the decomposition point of a lanthanide coordination polymer with glutaric acid is over 300 °C [9]. However, their emission quantum yields have been extremely low, because their coordination polymers are attributed to the nonradiative transition via vibrational relaxation of high-vibrational frequency O–H bonds in polymer structure [10, 11]. Luminescent coordination polymer with both high thermostability and emission quantum efficiency is required as a novel luminophore in the field of future opto-electronic devices.

Here, the author considers that the introduction of low-vibrational frequency (LVF) ligands as a linker part in the polymer chains would result in the preparation of a lanthanide coordination polymer with strong luminescence properties. Strongly luminescent lanthanide complexes composed of LVF hfa and bidentate phosphine oxide ligands have been described in former chapters. The author also proposes that the introduction of aromatic aryl groups in the linker part of lanthanide coordination polymer is effective for the construction of thermostable luminophores with intermolecular interactions, such as CH/F, π–π, and CH/π interactions.

In this chapter, the author reports on novel coordination polymers composed of Eu(III) ion and 4 types of aryl units; $[Eu(hfa)_3(dpb)]_n$, $[Eu(hfa)_3(dpbp)]_n$, $[Eu(hfa)_3(dpbt)]_n$, and $[Eu(hfa)_3(dppcz)]_n$ (dpb: 1,4-bis(diphenylphosphoryl) benzene, dpbp: 4,4′-bis(diphenylphosphoryl)biphenyl, dpbt: 4,4′-bis(diphenylphos phoryl)bithiophene, dppcz: 3,6-bis(diphenylphosphoryl)-9-phenylcarbazole) as shown in Fig. 2.1. Their thermal stabilities and luminescence properties are characterized by

K. Miyata, *Highly Luminescent Lanthanide Complexes with Specific Coordination Structures*, Springer Theses,
DOI: 10.1007/978-4-431-54944-4_2, © Springer Japan 2014

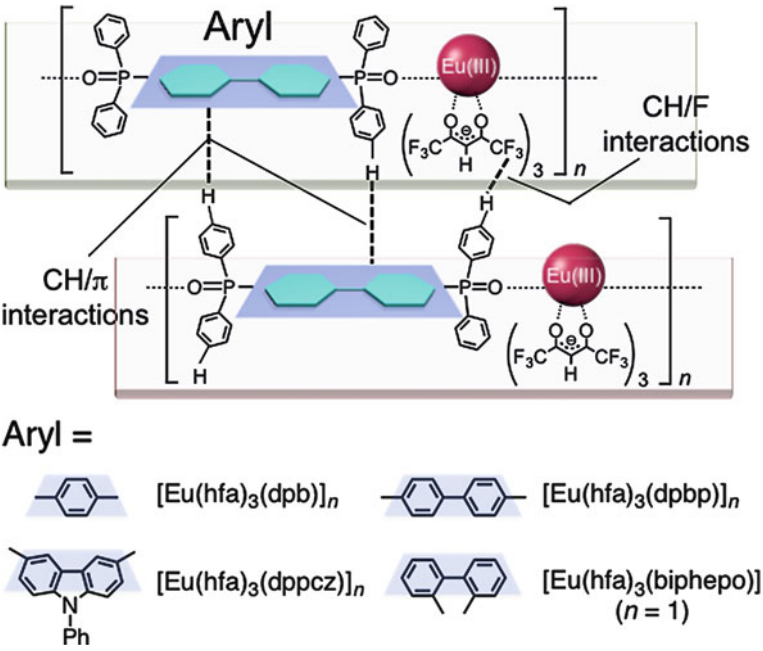

Fig. 2.1 Chemical structures of Eu(III) coordination polymers developed in this study

the thermogravimetric analyses (TGA and DSC), emission quantum yields, emission lifetimes, photosensitized energy transfer efficiency, and the nonradiative rate constants. In particular, $[Eu(hfa)_3(dppcz)]_n$ has both thermal stability (decomposition point =300 °C) and a high emission quantum yield ($\Phi_{Ln} = 83$ % in the solid state). Novel luminophores with heat durability are expected to open up new fields of material chemistry.

2.2 Experimental Section

2.2.1 General

The starting materials, 1,4-difluorobenzene (TCI, >95 %), 4,4′-dibromobiphenyl (TCI, >98 %), 2,2′-bithiophene (TCI, >98 %), 3,6-dibromo-9-phenylcarbazole (TCI, >98 %) were used as received. All other chemicals were reagent grade and were used without further purification. All reactions involving air- and moisture-sensitive reagents were carried out under an argon atmosphere using dried solvents. Synthetic routes of organic ligands are shown in Scheme 2.1. The preparation method of $[Eu(hfa)_3(H_2O)_2]$ was described in Chap 5. Infrared spectra were recorded on a JASCO FT/IR–350 spectrometer. ^{1}H NMR spectra were recorded on a

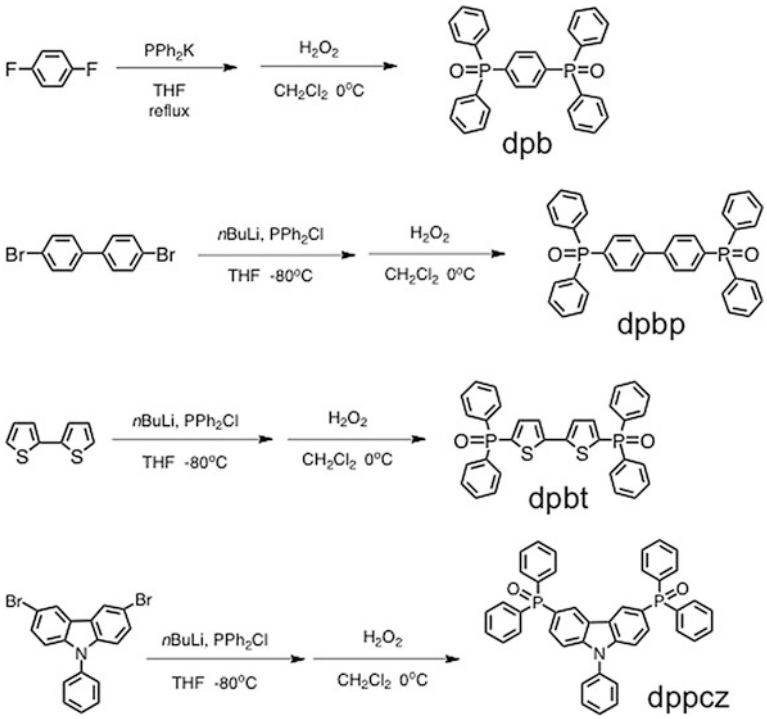

Scheme 2.1 Synthetic routes of organic ligands of Eu(III) coordination polymers

JEOL JNM-EX270 (270 MHz). ^{1}H NMR chemical shifts were determined by tetramethylsilane (TMS) as an internal standard. Elemental analysis and mass spectrometry were performed at the Instrumental Analysis Division in Hokkaido University. Thermogravimetric analysis was performed on a Rigaku TermoEvo TG8120 analyzer in an argon atmosphere at a heating rate of 1 °C min^{-1}. DSC measurement was performed on a MAC DSC3220 at a heating rate of 1 °C min^{-1}.

2.2.2 Syntheses

2.2.2.1 Preparation of 1,4-bis(diphenylphosphoryl)benzene (dpb)

1,4-bis(diphenylphosphoryl)benzene was synthesized according to the published procedure [12]. A solution of 1,4-difluorobenzene (0.80 mL, 8.0 mmol) was added dropwise to a solution of potassium diphenylphosphide (40 mL, 0.5 M THF, 20 mmol). The mixture was allowed to stir for 1 h and then was brought to reflux for 12 h. THF was removed under reduced pressure, and methanol (*ca.* 40 mL) was added. The mixture was then heated to reflux for 30 min. A gray precipitate

was formed, after which the methanol was decanted off. The obtained gray solid and dichloromethane (20 mL) were placed in a flask. The solution was cooled to 0 °C and then 30 % H_2O_2 aqueous solution (5 mL) was added to it. The reaction mixture was stirred for 2 h. The product was extracted with dichloromethane, the extracts washed with brine for three times and dried over anhydrous $MgSO_4$. The solvent was evaporated to afford a white powder. Recrystallization from dichloromethane for gave white crystals of the titled compound.

Yield: 2.5 g (66 %). ^{1}H NMR (270 MHz, $CDCl_3$, 25 °C) δ 7.48–7.78 (m, 24H; P-C_6H_5, C_6H_4) ppm. ESI–Mass (m/z) = 479.1 $[M+H]^+$. Anal. Calcd for $C_{30}H_{24}O_2P_2$: C, 75.31; H, 5.06. Found: C, 74.86; H, 5.11.

2.2.2.2 Preparation of 4,4′-bis(diphenylphosphoryl)biphenyl (dpbp)

4,4′-bis(diphenylphosphoryl)biphenyl was synthesized according to the published procedure [13–15]. A solution of *n*-BuLi (9.3 mL, 1.6 M hexane, 15 mmol), was added dropwise to a solution of 4,4′-dibromobiphenyl (1.9 g, 6.0 mmol) in dry THF (30 mL) at –80 °C. The addition was completed in *ca.* 15 min during which time a yellow precipitate was formed. The mixture was allowed to stir for 3 h at –10 °C, after which a PPh_2Cl (2.7 mL, 15 mmol) was added dropwise at –80 °C. The mixture was gradually brought to room temperature, and stirred for 14 h. The product was extracted with ethyl acetate, the extracts washed with brine for three times and dried over anhydrous $MgSO_4$. The solvent was evaporated, and resulting residue was washed with acetone and ethanol for several times. The obtained white solid and dichloromethane (40 mL) were placed in a flask. The solution was cooled to 0 °C and then 30 % H_2O_2 aqueous solution (5 mL) was added to it. The reaction mixture was stirred for 2 h. The product was extracted with dichloromethane, the extracts washed with brine for three times and dried over anhydrous $MgSO_4$. The solvent was evaporated to afford a white powder. Recrystallization from dichloromethane gave white crystals of the titled compound.

Yield: 1.7 g (54 %). IR (KBr): 1120 (st, P=O) cm^{-1}. ^{1}H NMR (270 MHz, $CDCl_3$, 25 °C) δ 7.67–7.80 (m, 16H; P-C_6H_5, C_6H_4), 7.45–7.60 (m, 12H; P-C_6H_5, C_6H_4) ppm. ESI–Mass (m/z) = 555.2 $[M+H]^+$. Anal. Calcd for $C_{36}H_{28}O_2P_2$: C, 77.97; H, 5.09. Found: C, 77.49; H, 5.20.

2.2.2.3 Preparation of 4,4′-bis(diphenylphosphoryl)bithiophene (dpbt)

A solution of *n*-BuLi (13 mL, 1.6 M hexane, 20 mmol), was added dropwise to a solution of 2,2′-bithiophene (1.2 g, 7.2 mmol) in dry THF (20 mL) at –80 °C. The addition was completed in *ca.* 15 min during which time a yellow precipitate was formed. The mixture was allowed to stir for 3 h at –10 °C, after which a PPh_2Cl (3.7 mL, 20 mmol) was added dropwise at –80 °C. The mixture was gradually brought to room temperature, and stirred for 18 h. The product was extracted with ethyl acetate, the extracts washed with brine for three times and dried over

anhydrous $MgSO_4$. The solvent was evaporated, and resulting residue was washed with methanol for several times. The obtained yellow solid and dichloromethane (40 mL) were placed in a flask. The solution was cooled to 0 °C and then 30 % H_2O_2 aqueous solution (10 mL) was added to it. The reaction mixture was stirred for 2 h. The product was extracted with dichloromethane, the extracts washed with brine for three times and dried over anhydrous $MgSO_4$. The solvent was evaporated to afford a yellow powder. Recrystallization from dichloromethane gave yellow crystals of the titled compound.

Yield: 1.4 g (31 %). IR (KBr): 1122 (st, P=O) cm^{-1}. ^1H NMR (270 MHz, $CDCl_3$, 25 °C) δ 7.45–7.79 (m, 20H; P-C_6H_5), 7.33–7.37 (m, 2H; C_4H_2S), 7.24–7.27 (m, 2H; C_4H_2S) ppm. ESI–Mass (*m/z*) = 567.1 $[M+H]^+$. Anal. Calcd for $C_{32}H_{24}O_2P_2S_2$: C, 67.83; H, 4.27. Found: C, 67.13; H, 4.40.

2.2.2.4 Preparation of 3,6-bis(diphenylphosphoryl)-9-phenylcarbazole (dppcz)

A solution of *n*-BuLi (8.8 mL, 1.6 M hexane, 14 mmol), was added dropwise to a solution of 3,6-dibromo-9-phenylcarbazole (2.4 g, 6.0 mmol) in dry THF (30 mL) at –80 °C. The addition was completed in *ca.* 10 min during which time a white yellow precipitate was formed. The mixture was allowed to stir for 2 h at –10 °C, after which a PPh_2Cl (2.6 mL, 14 mmol) was added dropwise at –80 °C. The mixture was gradually brought to room temperature, and stirred for 18 h to give a white precipitate. The precipitate was filtered, washed with methanol for several times, and dried in vacuo. The obtained white powder and dichloromethane (40 mL) were placed in a flask. The solution was cooled to 0 °C and then 30 % H_2O_2 aqueous solution (8 mL) was added to it. The reaction mixture was stirred for 2 h. The product was extracted with dichloromethane, the extracts washed with brine for three times and dried over anhydrous $MgSO_4$. The solvent was evaporated to afford a white powder. Recrystallization from dichloromethane/hexane gave colorless crystals of the titled compound. Yield: 2.0 g (53 %). IR (KBr): 1122 (st, P=O) cm^{-1}. ^1H NMR (270 MHz, $CDCl_3$, 25 °C) δ 8.43–8.47 (d, J = 10.8 Hz, 2H; P-C_6H_5), 7.63–7.76 (m, 11H; C_4H_2S), 7.43–7.60 (m, 18H; C_4H_2S) ppm. ESI–Mass (*m/z*) = 644.2 $[M+H]^+$. Anal. Calcd for $C_{43}H_{31}NO_2P_2$: C, 78.37; H, 4.85; N, 2.18. Found: C, 78.42; H, 5.00; N, 2.18.

2.2.2.5 General Procedure for the Preparation of Eu(III) Coordination Polymers

Phosphine oxide ligand (1 equiv.) and $[Eu(hfa)_3(H_2O)_2]$ (1 equiv.) were dissolved in chloroform–methanol. The solution was refluxed while stirring for 8 h, and the reaction mixture was concentrated to dryness. A single crystal suitable for X-ray structural determination of Eu(III) coordination polymer was obtained by the diffusion method of methanol–chloroform solution at room temperature.

[Eu(hfa)$_3$(dpb)]$_n$. Yield: 65 mg (42 %; for monomer). IR (KBr): 1652 (st, C=O), 1256–1145 (st, C–F), 1128 (st, P=O) cm^{-1}. ESI–Mass (*m/z*) = 1045.05 [Eu(hfa)$_2$(dpb)]$^+$, 2297.18 [Eu$_2$(hfa)$_5$(dpb)$_2$]$^+$. Anal. Calcd for [$C_{45}H_{27}EuF_{18}O_8P_2]_n$: C, 43.18; H, 2.17. Found: C, 43.12; H 2.28.

[Eu(hfa)$_3$(dpbp)]$_n$. Yield: 98 mg (67 %; for monomer). IR (KBr): 1653 (st, C=O), 1255–1145 (st, C–F), 1127 (st, P=O) cm^{-1}. ESI–Mass (*m/z*) = 1120.08 [Eu(hfa)$_2$(dpbp)]$^+$, 2447.15 [Eu$_2$(hfa)$_5$(dpbp)$_2$]$^+$. Anal. Calcd for [$C_{51}H_{31}EuF_{18}O_8P_2]_n$: C, 46.14; H, 2.35. Found: C, 45.59; H 2.49.

[Eu(hfa)$_3$(dpbt)]$_n$. Yield: 160 mg (68 %; for monomer). IR (KBr): 1651 (st, C=O), 1254–1145 (st, C–F), 1128 (st, P=O) cm^{-1}. ESI–Mass (*m/z*) = 1133.00 [Eu(hfa)$_2$(dpbt)]$^+$, 2473.02 [Eu$_2$(hfa)$_5$(dpbt)$_2$]$^+$. Anal. Calcd for [$C_{47}H_{27}EuF_{18}O_8P_2S_2]_n$: C, 42.14; H, 2.03. Found: C, 42.67; H 2.12.

[Eu(hfa)$_3$(dppcz)]$_n$. Yield: 110 mg (50 %; for monomer). IR (KBr): 1652 (st, C=O), 1256–1145 (st, C–F), 1128 (st, P=O) cm^{-1}. ESI–Mass (*m/z*) = 1210.13, [Eu(hfa)$_2$(dppcz)]$^+$, 1853.34, [Eu(hfa)$_2$(dppcz)$_2$]$^+$. Anal. Calcd for [$C_{57}H_{34}EuF_{18}NO_8P_2]_n$: C, 48.32; H, 2.42; N, 0.99. Found: C, 47.95; H, 2.77; N, 1.06.

2.2.3 Crystallography

Colorless single crystals of Eu(III) coordination polymers were mounted on a glass fiber using paraffin oil. All measurements were made on a Rigaku Mercury CCD area detector with graphite monochromated Mo-Kα radiation. All structures were solved by direct methods (SIR 2004) [16] and expanded using Fourier techniques. The non-hydrogen atoms were refined anisotropically. Hydrogen atoms were refined using the riding model. All calculations were performed using the Crystal Structure crystallographic software package except for refinement, which was performed using SHELXL-97 [17]. The author confirmed the CIF data using the check CIF/PLATON service.

2.2.4 Optical Measurements

Emission spectra of Eu(III) coordination polymers were measured on a JASCO F-6300-H spectrometer and corrected for the response of the detector system. Emission lifetimes (τ_{obs}) were measured using the third harmonics (355 nm) of a Q-switched Nd:YAG laser (Spectra Physics, INDI-50, fwhm = 5 ns, λ = 1064 nm) and a photomultiplier (Hamamatsu photonics, R5108, response time $\leq$1.1 ns). The Nd:YAG laser response was monitored with a digital oscilloscope (Sony Tektronix, TDS3052, 500 MHz) synchronized to the single-pulse excitation. Emission lifetimes were determined from the slope of logarithmic plots of the decay profiles. The emission quantum yields excited at 380 nm (Φ_{tot}) were estimated using JASCO F-6300-H spectrometer attached with JASCO ILF-533 integrating sphere unit

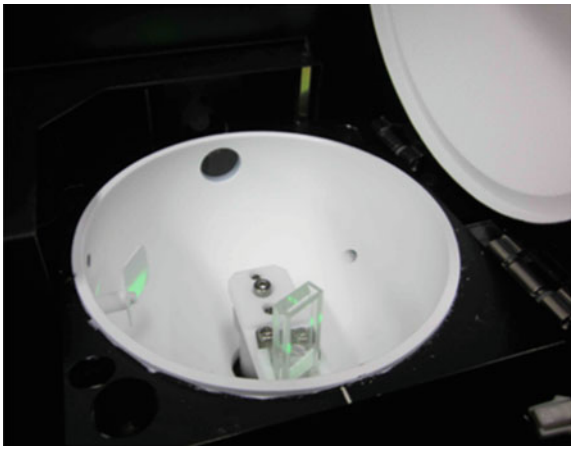

Fig. 2.2 JASCO ILF-533 integrating sphere unit

($\phi = 100$ mm, Fig. 2.2). The wavelength dependences of the detector response and the beam intensity of Xe light source for each spectrum were calibrated using a standard light source.

The photophysical properties of the Eu(III) coordination polymers in the solid state were investigated from estimation of the 4f–4f emission quantum yields (Φ_{Ln}), and the radiative (k_{r}) and nonradiative (k_{nr}) rate constants from the radiative (τ_{rad}) and observed lifetimes (τ_{obs}). The radiative lifetime is defined as an ideal emission lifetime without nonradiative processes. The radiative and observed lifetimes are expressed by

$$\tau_{rad} = \frac{1}{k_r} \tag{2.1}$$

$$\tau_{obs} = \frac{1}{k_r + k_{nr}} \tag{2.2}$$

Φ_{Ln}, k_{r}, and k_{nr} of the Eu(III) compounds are given by

$$\Phi_{Ln} = \frac{k_r}{k_r + k_{nr}} = \frac{\tau_{obs}}{\tau_{rad}} \tag{2.3}$$

$$\frac{1}{\tau_{rad}} = A_{MD,0} n^3 \left(\frac{I_{tot}}{I_{MD}} \right) \tag{2.4}$$

$$k_r = \frac{1}{\tau_{rad}} \tag{2.5}$$

$$k_{nr} = \frac{1}{\tau_{obs}} - \frac{1}{\tau_{rad}} \tag{2.6}$$

where $A_{MD,0}$ is the spontaneous emission probability for the $^5D_0$–$^7F_1$ transition in vacuo (14.65 s^{-1}), n is the refractive index of the medium (an average index of refraction equal to 1.5 was employed [18]), and (I_{tot}/I_{MD}) is the ratio of the total area of the corrected Eu(III) emission spectrum to the area of the $^5D_0$–$^7F_1$ band.

2.3 Results and Discussion

2.3.1 Coordination and Network Structures

Single crystals of Eu(III) coordination polymers with phosphine oxides, $[Eu(hfa)_3(dpb)]_n$, $[Eu(hfa)_3(dpbp)]_n$, $[Eu(hfa)_3(dpbt)]_n$, and $[Eu(hfa)_3(dppcz)]_n$ were successfully prepared for X-ray single crystal analyses by the diffusion method using methanol–chloroform solutions. The resulting crystal data are summarized in Fig. 2.3 and Table 2.1. The ORTEP views show that the phosphine oxide ligand acts as a bidentate bridge between lanthanide ions in one-dimensional polymeric chains. The coordination sites of $[Eu(hfa)_3(dpb)]_n$, $[Eu(hfa)_3(dpbp)]_n$, $[Eu(hfa)_3(dpbt)]_n$, and $[Eu(hfa)_3(dppcz)]_n$ comprise three hfa ligands and two phosphine oxide units. Their structures are categorized as an octa-coordinated square antiprism with no inverted center in the crystal field, so that enhancement of their luminescence properties is expected with allowed electronic transition probabilities [19, 20].

Selected bond lengths between Eu(III) ions and oxygen atoms in coordination sites (Eu–O and Eu–Eu distances) are summarized in Table 2.2. The Eu–Eu distances of $[Eu(hfa)_3(dpb)]_n$, $[Eu(hfa)_3(dpbp)]_n$, $[Eu(hfa)_3(dpbt)]_n$, and $[Eu(hfa)_3(dppcz)]_n$ were determined 9.91, 10.36, 10.60, and 11.76 Å, respectively. These distances may be longer than the critical distance for nonradiative dipole-dipole energy transfer between Eu(III) ions. Average Eu–O distances between Eu(III) ions and oxygen atoms of phosphine oxide ligands in $[Eu(hfa)_3(dpb)]_n$, $[Eu(hfa)_3(dpbp)]_n$, $[Eu(hfa)_3(dpbt)]_n$ and $[Eu(hfa)_3(dppcz)]_n$ were estimated to be 2.31, 2.32, 2.31, and 2.30 Å, respectively, which are shorter than the Eu–O distances of hfa ligands in $[Eu(hfa)_3(dpb)]_n$ (2.41 Å), $[Eu(hfa)_3(dpbp)]_n$ (2.42 Å), $[Eu(hfa)_3(dpbt)]_n$ (2.41 Å), and $[Eu(hfa)_3(dppcz)]_n$ (2.42 Å). These results indicate that the coordination ability of phosphine oxide is stronger than that of the hfa ligands. The strong coordination ability of phosphine oxide in Eu(III) complexes has been reported. The tight-coordination of phosphine oxide molecules with low vibrational frequency (P=O: 1120 cm^{-1}) prevents coordination of high-vibrational molecules such as water, which results in enhancement of their luminescence properties.

X-ray analyses also reveal intermolecular interactions between one-dimensional polymeric chains (Fig. 2.4). Two CH/F interactions in one unit were identified for $[Eu(hfa)_3(dpb)]_n$, $[Eu(hfa)_3(dpbp)]_n$, $[Eu(hfa)_3(dpbt)]_n$, and $[Eu(hfa)_3(dppcz)]_n$. Remarkable CH/π interactions in the polymer chains of $[Eu(hfa)_3(dpbp)]_n$,

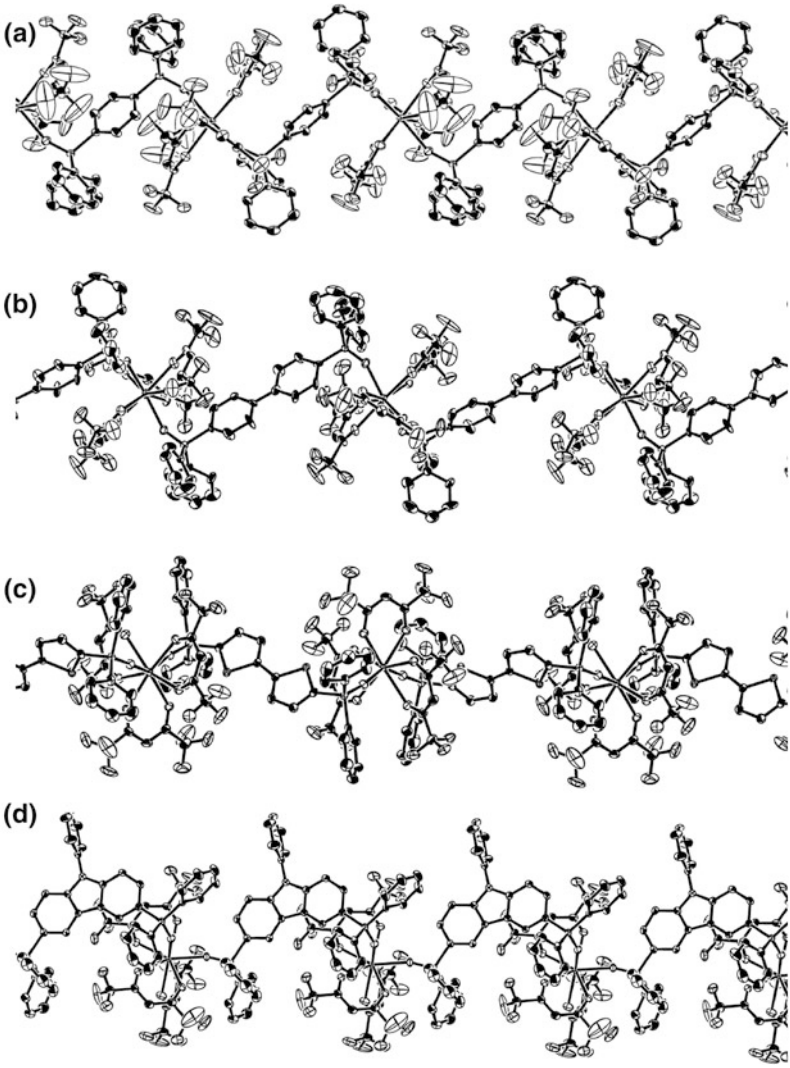

Fig. 2.3 ORTEP drawings (showing 50 % probability displacement ellipsoids) of **a** $[Eu(hfa)_3(dpb)]_n$, **b** $[Eu(hfa)_3(dpbp)]_n$, **c** $[Eu(hfa)_3(dpbt)]_n$, and **d** $[Eu(hfa)_3(dppcz)]_n$

$[Eu(hfa)_3(dpbt)]_n$, and $[Eu(hfa)_3(dppcz)]_n$ were observed. The author considers that tight-binding structures composed of Eu(III) ions and phosphine oxide result in the excellent thermogravimetric and emission properties.

Table 2.1 Crystal data of Eu(III) coordination polymers

	$[Eu(hfa)_3(dpb)]_n$	$[Eu(hfa)_3(dpbp)]_n$	$[Eu(hfa)_3(dpbt)]_n$	$[Eu(hfa)_3(dppcz)]_n$
Chemical formula	$C_{45}H_{27}F_{18}O_8P_2Eu$	$C_{52}H_{31}F_{18}O_8P_2Eu$	$C_{47}H_{27}F_{18}O_8P_2S_2Eu$	$C_{57}H_{34}F_{18}NO_8P_2Eu$
Formula weight	1251.58	1339.69	1339.72	1416.78
Crystal color, habit	Colorless, prism	Colorless, prism	Colorless, prism	Colorless, prism
Crystal system	Triclinic	Monoclinic	Monoclinic	Monoclinic
Space group	*P*-1 (#2)	*C*2/*c* (#15)	*C*2/*c* (#15)	$P2_1/n$ (#14)
a/Å	12.610(3)	23.477(4)	22.786(2)	12.3580(14)
b/Å	13.622(3)	13.367(2)	13.6381(8)	21.170(2)
c/Å	15.282(3)	17.168(3)	17.0846(11)	22.482(3)
α/deg	71.928(8)			
β/deg	79.279(9)	97.5749(8)	103.0178(15)	99.6974(5)
γ/deg	81.346(9)			
V/Å^3	2439.9(9)	5340.5(16)	5172.8(7)	5797.6(11)
Z	2	4	4	4
d_{calc}/g cm^{-3}	1.703	1.666	1.720	1.623
T/°C	−123 ± 1	−123 ± 1	−123 ± 1	−123 ± 1
μ (Mo Kα)/cm^{-1}	14.676	13.472	14.685	12.465
Max 2θ/deg	55.0	55.0	55.0	55.0
No. of measured reflections	19890	21091	20459	45925
No. of unique reflections	10984	6099	5928	13215
R ($I > 2\sigma(I)$)[a]	0.0335	0.0266	0.0258	0.0319
R_w ($I > 2\sigma(I)$)[b]	0.0949	0.0668	0.0689	0.0796

[a] $R = \Sigma \, ||F_o| - |F_c|| / \Sigma \, |F_o|$

[b] $R_w = [(\Sigma \, w \, (|F_o| - |F_c|)^2 / \Sigma \, w \, F_o^2)]^{1/2}$

Table 2.2 Selected bond lengths (Å) of Eu(III) coordination polymers

Bond	$[Eu(hfa)_3(dpb)]_n$	$[Eu(hfa)_3(dpbp)]_n$	$[Eu(hfa)_3(dpbt)]_n$	$[Eu(hfa)_3(dppcz)]_n$
Eu−O1 (P=O)	2.307	2.319	2.314	2.321
Eu−O2 (P=O)	2.312	2.319	2.314	2.284
Average bond length	2.310	2.319	2.314	2.303
Eu−O3 (C=O)	2.457	2.416	2.407	2.420
Eu−O4 (C=O)	2.362	2.423	2.413	2.404
Eu−O5 (C=O)	2.407	2.411	2.407	2.408
Eu−O6 (C=O)	2.409	2.411	2.413	2.446
Eu−O7 (C=O)	2.424	2.416	2.398	2.392
Eu−O8 (C=O)	2.399	2.423	2.398	2.445
Average bond length	2.410	2.417	2.406	2.419
Eu−Eu	9.910	10.367	10.602	11.755

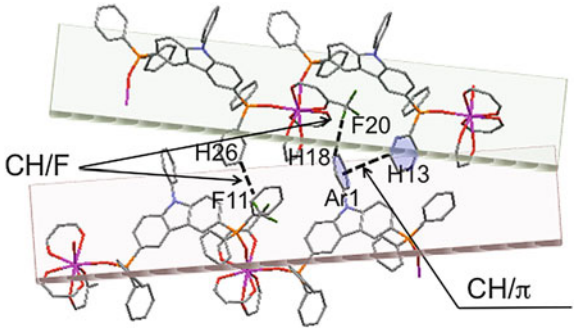

Fig. 2.4 Crystal structures of $[Eu(hfa)_3(dppcz)]_n$ focused on the intermolecular interactions between one-dimensional polymeric chains. *Dashed lines* denote CH/F and CH/π interactions. Two CH/F interactions ($d_{CH/F} = 2.62$ Å (H18–F20), 2.74 Å (H26–F11)) and one CH/π interaction ($d_{CH/\pi} = 3.07$ Å (H13–Ar1)) are displayed

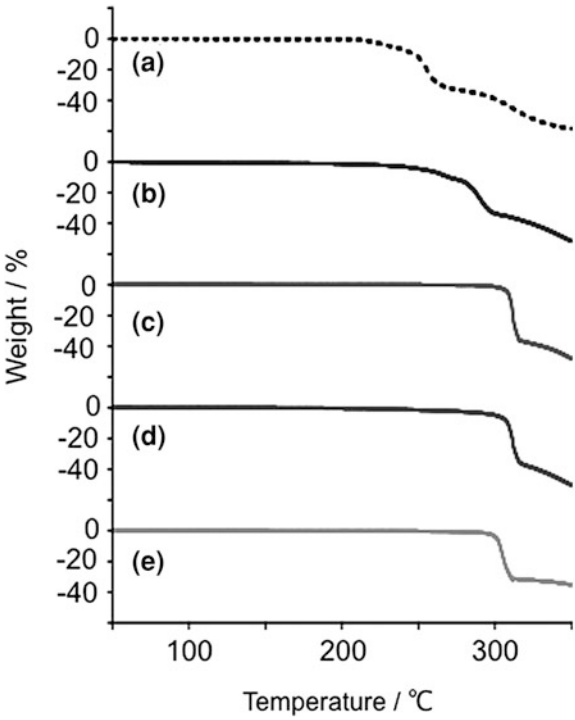

Fig. 2.5 TGA thermograms of **a** $[Eu(hfa)_3(biphepo)]$, **b** $[Eu(hfa)_3(dpb)]_n$, **c** $[Eu(hfa)_3(dpbp)]_n$, **d** $[Eu(hfa)_3(dpbt)]_n$, and **e** $[Eu(hfa)_3(dppcz)]_n$ under an argon atmosphere

2.3.2 Thermal Analyses

To estimate the thermal stability of Eu(III) coordination polymers, TGA and DSC were conducted. Decomposition points from the TGA thermograms are 261, 308, and 300 °C for $[Eu(hfa)_3(dpb)]_n$, $[Eu(hfa)_3(dpbp)]_n$, and $[Eu(hfa)_3(dppcz)]_n$, respectively (Fig. 2.5). In contrast, the decomposition point of the reported Eu(III) complex, $[Eu(hfa)_3(biphepo)]$ (biphepo: 2,2′-bis(diphenylphosphoryl)biphenyl),

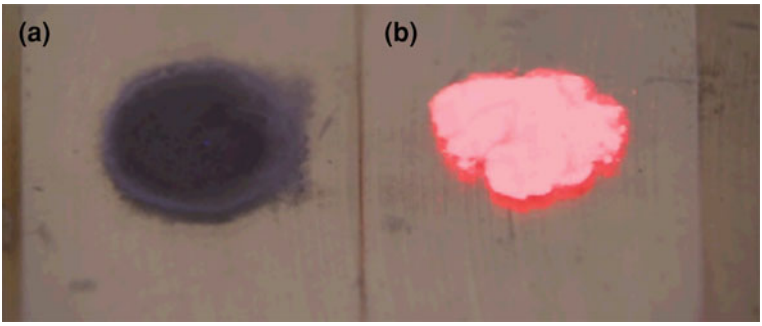

Fig. 2.6 Photographs of **a** [Eu(hfa)$_3$(biphepo)] and **b** [Eu(hfa)$_3$(dpbp)]$_n$ after heating at 300 °C for 10 min under UV irradiation

was found to be 230 °C. The high thermal stability of [Eu(hfa)$_3$(dpbp)]$_n$ and [Eu(hfa)$_3$(dppcz)]$_n$ might be due to their tight-binding structures supported by a combination of CH/F and CH/π interactions (Fig. 2.4). The binding energies of CH/F (hydrogen bond) and CH/π interactions are generally known to be 10–30 and 2–10 kJ mol^{-1}, respectively [21]. The author considers that a combination of both CH/F and CH/π interactions in coordination polymers is effective for the construction of thermostable luminophore compounds. As displayed in Fig. 2.6, [Eu(hfa)$_3$(dpbp)]$_n$ after heating at 300 °C for 10 min exhibits brilliant red luminescence under UV irradiation (excitation at 365 nm), whereas [Eu(hfa)$_3$(biphepo)] does not emit photons owing to thermal decomposition at 230 °C. The enhanced photostability of organic molecules containing hydrogen bonds has been reported [22]. In the author's system, high photostability of [Eu(hfa)$_3$(dpbp)]$_n$ has been also observed under UV irradiation. The DSC thermograms of [Eu(hfa)$_3$(dpb)]$_n$, [Eu(hfa)$_3$ (dpbp)]$_n$, and [Eu(hfa)$_3$(dppcz)]$_n$ show that exothermic peaks based on the decomposition points and endothermic peaks corresponding to melting points were observed (Fig. 2.7). Thus, the Eu(III) coordination polymers exhibit thermal behavior similar to polymer compounds.

2.3.3 Photophysical Properties

Steady-state emission spectra of the Eu(III) coordination polymers in the solid state are shown in Fig. 2.8 (right). Emission bands were observed at around 578, 591, 613, 650, and 698 nm, and are attributed to the f–f transitions of $^5D_0$–^7F_J with $J = 0$, 1, 2, 3, and 4, respectively. The emission band at 613 nm ($^5D_0$–$^7F_2$) is due to electric dipole transitions, which is strongly dependent on the coordination geometry. Their time-resolved emission profiles revealed single-exponential decays with millisecond scale lifetimes. The observed emission lifetimes from $^5D_0$ excited level (τ_{obs}) were determined from the slopes of logarithmic decay profiles. The emission lifetimes of [Eu(hfa)$_3$(dpb)]$_n$, [Eu(hfa)$_3$(dpbp)]$_n$, and [Eu(hfa)$_3$ (dppcz)]$_n$ were determined to be 0.93, 0.85, and 0.93 ms, respectively (Fig. 2.9).

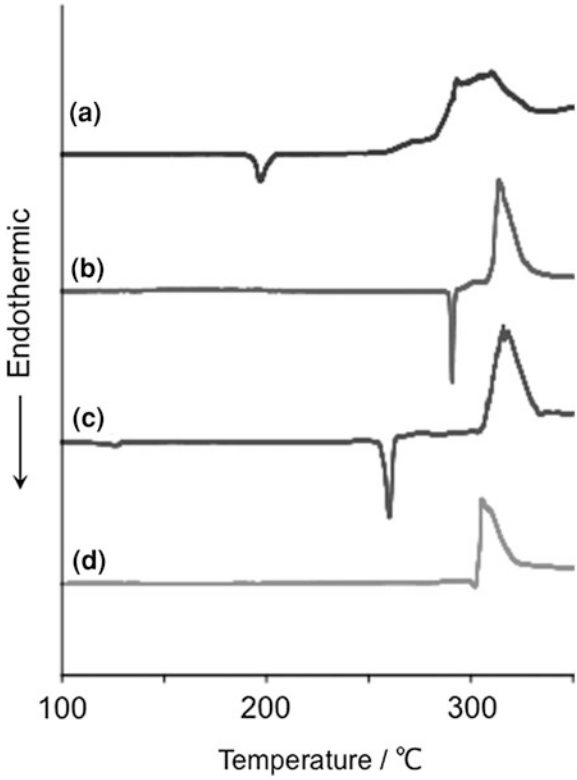

Fig. 2.7 DSC thermograms of **a** $[Eu(hfa)_3(dpb)]_n$, **b** $[Eu(hfa)_3(dpbp)]_n$, **c** $[Eu(hfa)_3(dpbt)]_n$, and **d** $[Eu(hfa)_3(dppcz)]_n$

The photophysical properties of the Eu(III) coordination polymers in the solid state are summarized in Table 2.3. The 4f–4f emission quantum yields (Φ_{Ln}) [18, 23, 24] for $[Eu(hfa)_3(dpb)]_n$, $[Eu(hfa)_3(dpbp)]_n$, and $[Eu(hfa)_3(dppcz)]_n$ were estimated to be 70, 72, and 83 %, respectively. These quantum yields are approximately four times larger than that for $[Eu(hfa)_3(H_2O)_2]$ [25, 26], and similar to that reported for [Eu(hfa)$_3$(biphepo)] (Φ_{Ln} = 73 % in the solid state), which have been reported as high luminescent Eu(III) complexes. According to the photosensitized energy transfer efficiency (η_{sens}) calculated from Φ_{Ln} (excited at 465 nm) and Φ_{tot} (excited at 380 nm), $[Eu(hfa)_3$ (dppcz)$]_n$ are approximately five times larger than that for reported $[Eu(hfa)_3(H_2O)_2]$. Since absorption band at 380 nm is assigned to a π–π^* transition of hfa ligand (Fig. 2.8 left), these results suggest that the photosensitized energy transfer from hfa ligands to Eu(III) ions is enhanced in the coordination polymers, in particular, $[Eu(hfa)_3(dppcz)]_n$.

The nonradiative rate constants (k_{nr}) for the Eu(III) coordination polymers ($1.8–3.3 \times 10^2$ s^{-1}) were approximately ten times smaller than that for $[Eu(hfa)_3(H_2O)_2]$ (3.7×10^3 s^{-1}). The smaller k_{nr} for the Eu(III) coordination polymers is attributed to the structural rigidity and low-vibrational frequencies in the crystal lattice. Our research group has previously reported that the nonradiative

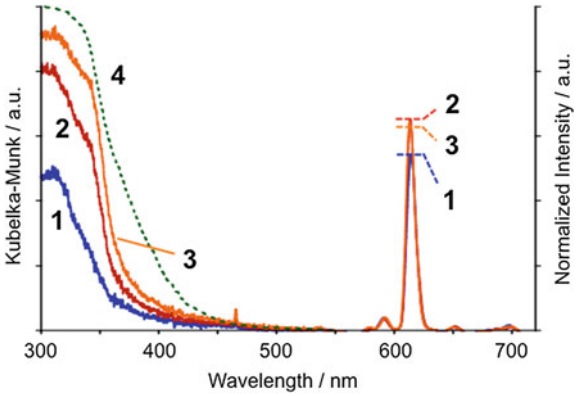

Fig. 2.8 Left: Diffuse-reflectance absorption spectra of $[Eu(hfa)_3(dpb)]_n$ (*line 1*), $[Eu(hfa)_3(dpbp)]_n$ (*line 2*), $[Eu(hfa)_3(dppcz)]_n$ (*line 3*), and $[Eu(hfa)_3(H_2O)_2]$ (*dot line 4*) in the solid state. The absorption bands at 310 nm are attributed to a π-π^* transition of the hfa lilgands. The small bands at 465 nm are assigned to the $^7F_{0-5}D_2$ transition in the Eu(III) ion. Right: Emission spectra of $[Eu(hfa)_3(dpbp)]_n$, $[Eu(hfa)_3(dppcz)]_n$, and $[Eu(hfa)_3(dpb)]_n$ in the solid state. Excitation wavelength is 465 nm. The spectra were normalized with respect to the magnetic dipole transition ($^5D_0$–$^7F_1$)

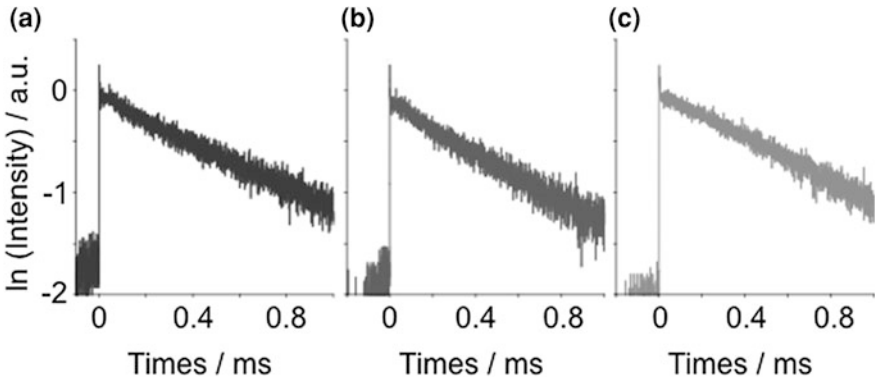

Fig. 2.9 The decay profiles of **a** $[Eu(hfa)_3(dpb)]_n$, **b** $[Eu(hfa)_3(dpbp)]_n$, and **c** $[Eu(hfa)_3(dppcz)]_n$ in the solid state

transitions of lanthanide complexes are caused by the high-vibrational frequency of O–H bonds, such as in water and alcohol. k_{nr} for $[Eu(hfa)_3(biphepo)]$ is similar to those of $[Eu(hfa)_3(dpb)]_n$, $[Eu(hfa)_3(dpbp)]_n$, and $[Eu(hfa)_3(dppcz)]_n$. We consider that introduction of the LVF phosphine oxide ligand as a linker part in the polymer chains is effective for preparation of luminophores with high thermal stabilities and emission quantum yields.

Table 2.3 Photophysical and thermal properties of Eu(III) compounds in the solid state

Compound	interaction[a]	Decomp. point/°C[b]	Photophysical properties						
			τ_{obs} / ms[c]	τ_{rad} / ms[d]	Φ_{Ln} /%[d]	Φ_{tot} /%[e]	η_{sens} / %[f]	k_r /s^{-1} [d]	k_{nr} /s^{-1} [d]
$[Eu(hfa)_3(H_2O)_2]$	–	220[g]	0.22[h]	1.1[h]	19[h]	2.6[h]	13[h]	8.8×10^2	3.7×10^3
$[Eu(hfa)_3(biphepo)]$	–	230	0.94	1.3	73	21	29	7.8×10^2	2.8×10^2
$[Eu(hfa)_3(dpb)]_n$	CH/F	261	0.93	1.3	70	31	44	7.5×10^2	3.3×10^2
$[Eu(hfa)_3(dpbp)]_n$	CH/F, CH/π	308	0.85	1.2	72	29	40	8.5×10^2	3.2×10^2
$[Eu(hfa)_3(dppcz)]_n$	CH/F, CH/π	300	0.93	1.1	83	53	64	8.9×10^2	1.8×10^2

[a] From X-ray single crystal analyses (Fig. 2.4)
[b] From TGA thermograms (Fig. 2.5)
[c] Emission lifetime (τ_{obs}) of the Eu(III) coordination polymer were measured by excitation at 355 nm (Nd:YAG 3ω)
[d] Calculation methods are described in Experimental section
[e] Total emission quantum yield (excitation at 380 nm)
[f] Photosensitized energy transfer efficiency $\eta_{sens} = \Phi_{tot} / \Phi_{Ln}$
[g] From Ref. [18]
[h] From Ref. [25]

Fig. 2.10 The conceptual diagram in Chap. 2

2.3.4 Conclusions

The thermostable luminophores composed of Eu(III) coordination polymers were successfully synthesized (Fig. 2.10). In particular, $[Eu(hfa)_3(dppcz)]_n$ exhibits both high emission quantum yields ($\Phi_{Ln} = 83$ %) and remarkable thermal stability (decomposition point =300 °C) due to a tight-binding structure composed of Eu(III) ions and low-vibrational phosphine oxide, although many types of

luminescent organic dyes are generally decomposed at temperatures under 200 °C. The emission quantum yields of the author's coordination polymers are similar to those of strong-luminescent coordination polymers in former chapters. Reported new luminophores are expected to employ in optics applications such as luminescent plastics, displays, and opto-electronic devices.

References

1. A. Thirumurugan, S.K. Pati, M.A. Greenc, S. Natarajan, J. Mater. Chem. **13**, 2937 (2003)
2. C. Daiguebonne, N. Kerbellec, O. Guillou, J.-C.G. Bünzli, F. Gumy, L. Catala, T. Mallah, N. Audebrand, Y. Geraut, K. Bernot, G. Calvez, Inorg. Chem. **47**, 3700 (2008)
3. K. Binnemans, Chem. Rev. **109**, 4283 (2009)
4. C. Marchal, Y. Filinchuk, X.-Y. Chen, D. Imbert, M. Mazzanti, Chem. Eur. J. **15**, 5273 (2009)
5. T.K. Prasad, M.V. Rajasekharan, Inorg. Chem. **48**, 11543 (2009)
6. J. Rocha, L.D. Carlos, F.A. Almeida Paz, D. Ananias, Chem. Soc. Rev. **40**, 926 (2011)
7. S.V. Eliseeva, D.N. Pleshkov, K.A. Lyssenko, L.S. Lepnev, J.-C.G. Bünzli, N.P. Kuzmina, Inorg. Chem. **49**, 9300 (2010)
8. F. Marchetti, C. Pettinari, A. Pizzabiocca, A.A. Drozdov, S.I. Troyanov, C.O. Zhuravlev, S.N. Semenov, Y.A. Belousov, I.G. Timokhin, Inorg. Chim. Acta **363**, 4038 (2010)
9. C. Wang, Y. Xing, Z. Li, J. Li, X. Zeng, M. Ge, S. Niu, J. Mol. Struct. **931**, 76 (2009)
10. Y. Hasegawa, Y. Kimura, K. Murakoshi, Y. Wada, J. Kim, N. Nakashima, T. Yamanaka, S. Yanagida, J. Phys. Chem. **100**, 10201 (1996)
11. Y. Hasegawa, K. Murakoshi, Y. Wada, J. Kim, N. Nakashima, T. Yamanaka, S. Yanagida, Chem. Phys. Lett. **260**, 173 (1996)
12. P.W. Miller, M. Nieuwenhuyzen, J.P.H. Charmant, S.L. James, Inorg. Chem. **47**, 8367 (2008)
13. J.S. Field, R.J. Haines, E.I. Lakoba, M.H. Sosabowski, J. Chem. Soc. Perkin Trans. **1**, 3352 (2001)
14. R.D. Myrex, C.S. Colbert, G.M. Gray, Organometallics **23**, 409 (2004)
15. I.O. Koshevoy, A.J. Karttunen, S.P. Tunik, M. Haukka, S.I. Selivanov, A.S. Melnikov, P.Y. Serdobintsev, M.A. Khodorkovskiy, T.A. Pakkanen, Inorg. Chem. **47**, 9478 (2008)
16. M.C. Burla, R. Caliandro, M. Camalli, B. Carrozzini, G.L. Cascarano, L.D. Caro, C. Giacovazzo, G. Polidori, R. Spagana, J. Appl. Crystallogr. **38**, 381 (2005)
17. G.M. Sheldrick, Acta Crystallogr. Sect. A: Found. Crystallogr **64**, 112 (2008)
18. R. Pavithran, N.S. Saleesh Kumar, S. Biju, M.L. P. Reddy, S., Jr. Alves, R.O. Freire, Inorg. Chem. **45**, 2184 (2006)
19. Y. Hasegawa, M. Yamamuro, Y. Wada, N. Kanehisa, Y. Kai, S. Yanagida, J. Phys. Chem. A **107**, 1697 (2003)
20. R.B. King, J. Am. Chem. Soc. **91**, 7211 (1969)
21. G.R. Desiraju, T. Steiner, *The Weak Hydrogen Bond in Structural Chemistry and Biology* (Oxford University Press, Oxford 1999)
22. P. Slavíček, M. Fárník, Phys. Chem. Chem. Phys. **13**, 12123 (2011)
23. M.H.V. Werts, R.T.F. Jukes, J.W. Verhoeven, Phys. Chem. Chem. Phys. **4**, 1542 (2002)
24. J.-C.G. Bünzli, S.V. Eliseeva, In Springer *Series on Fluorescence. Lanthanide Luminescence: Photophysical, Analytical and Biological Aspects*, Vol. 8 ed. by P. Hänninen, H. Härmä, (Springer Verlag: Berlin, 2010)
25. S.V. Eliseeva, M. Ryazanov, F. Gumy, S.I. Troyanov, L.S. Lepnev, J.-C.G. Bünzli, N.P. Kuzmina, Eur. J. Inorg. Chem. **23** 4809 (2006)
26. S.V. Eliseeva, D.N. Pleshkov, K.A. Lyssenko, L.S. Lepnev, J.-C.G. Bünzli, N.P. Kuzmina, Inorg. Chem. **50**, 5137 (2011)

http://www.springer.com/978-4-431-54943-7

Highly Luminescent Lanthanide Complexes with Specific Coordination Structures

Miyata, K.

2014, XIII, 91 p. 52 illus., 21 illus. in color., Hardcover
ISBN: 978-4-431-54943-7